JOURNAL OF BACTERIOLOGY, Sept. 2009, p. 5734–5742 Vol. 191, No. 18
0021-9193/09/$08.00+0 doi:10.1128/JB.00293-09

Kinematics of Intracellular Chlamydiae Provide Evidence for Contact-Dependent Development▽†

David P. Wilson,[1] Judith A. Whittum-Hudson,[2] Peter Timms,[3] and Patrik M. Bavoil[4]*

National Centre in HIV Epidemiology and Clinical Research, Faculty of Medicine, University of New South Wales, Level 2, 376 Victoria Street, Darlinghurst, Sydney, NSW 2010, Australia[1]; Department of Immunology and Microbiology, Wayne State University School of Medicine, 550 East Canfield Avenue, Detroit, Michigan 48201[2]; Institute of Health and Biomedical Innovation, Queensland University of Technology, Kelvin Grove Campus, Blamey Street and Musk Avenue, Brisbane, QLD 4001, Australia[3]; and Department of Microbial Pathogenesis, University of Maryland Dental School, 650 West Baltimore Street, Baltimore, Maryland 21201[4]

Received 4 March 2009/Accepted 5 June 2009

A crucial process of chlamydial development involves differentiation of the replicative reticulate body (RB) into the infectious elementary body (EB). We present experimental evidence to provide support for a contact-dependent hypothesis for explaining the trigger involved in differentiation. We recorded live-imaging of *Chlamydia trachomatis*-infected McCoy cells at key times during development and tracked the temporospatial trajectories of individual chlamydial particles. We found that movement of the particles is related to development. Early to mid-developmental stages involved slight wobbling of RBs. The average speed of particles increased sharply at 24 h postinfection (after the estimated onset of RB to EB differentiation). We also investigated a penicillin-supplemented culture containing EBs, RBs, and aberrantly enlarged, stressed chlamydiae. Near-immobile enlarged particles are consistent with their continued tethering to the chlamydial inclusion membrane (CIM). We found a significantly negative, nonlinear association between speed and size/type of particles, providing further support for the hypothesis that particles become untethered near the onset of RB to EB differentiation. This study establishes the relationship between the motion properties of the chlamydiae and developmental stages, whereby wobbling RBs gradually lose contact with the CIM, and RB detachment from the CIM is coincidental with the onset of late differentiation.

Members of the *Chlamydiaceae* are ubiquitous bacterial pathogens in humans and animals. While many primary chlamydial infections are asymptomatic or of limited severity, severe disease and the most serious sequelae are thought to be associated with chronic or persistent infection or repeat infections that may occur over years or decades. In the laboratory, cultured eukaryotic cells such as HEp-2 or McCoy cells and various animal models are used as suitable model systems for primary chlamydial infection. Under these optimized conditions, chlamydiae undergo a typical developmental cycle, which is highly conserved across the genus. Initial internalization of the infectious chlamydial elementary body (EB) particle occurs within the first 2 h, followed shortly by differentiation of the EB into the chlamydial replicative form, the reticulate body (RB). RBs are thought to multiply exponentially, replicating their DNA every 2 to 3 h for approximately 6 to 10 generations. At 16+ h postinfection (hpi), an unknown signal provokes the onset of RB to EB differentiation, whereby individual RBs engage in a cellular condensation process, progressing through a poorly defined intermediate body (IB) form and ending with the metabolically inactive but highly infectious EB, thereby closing the developmental "cycle." Unlike the initial differentiation step which can be reasonably well synchronized, the late differentiation step is always asynchronous. Indeed, few EBs can be observed in relatively young inclusions, while significant numbers of RBs can often be seen in late inclusions (for *C. trachomatis*, these stages occur at approximately 20 and 48 hpi, respectively). Another perennial observation is that RBs are often observed in association with the chlamydial inclusion membrane (CIM) (21, 22, 27, 37), the membrane of the parasitophorous vacuole that contains the chlamydiae and is derived from the host cell plasma membrane (14). This is further supported by various imaging methods including cryo-electron microscopy (14), indirect immunofluorescence, confocal electron microscopy, and Nomarski differential interference contrast imaging (10, 15, 16, 31).

Models for persistent or chronic infection have also been established both in vitro and in animal models. Under conditions that induce a classical stress response in many bacteria, such as exposure to gamma interferon (3) or penicillin (23, 34), infection with phage (18), or deprivation of iron (30) or amino acids (9), chlamydial RBs undergo a dramatic morphological change to nondividing, aberrantly enlarged RBs (termed maxiRBs or mRBs) that will not differentiate into EBs (3, 23, 30, 34). Coincidental to the morphological change, expression of stress response genes is upregulated (e.g., hsp60) while expression of genes thought to be involved in late differentiation (e.g., *omcB*) is blocked (5, 6, 13). Because mRBs may be kept in culture for several weeks (except for phage-induced stress) and removal of the stressor "unlocks" development and allows re-

* Corresponding author. Mailing address: Department of Microbial Pathogenesis, University of Maryland Dental School, 650 W. Baltimore St., Baltimore, MD 21201. Phone: (410) 706-6789. Fax: (410) 706-0865. E-mail: pbavoil@umaryland.edu.

† Supplemental material for this article may be found at http://jb.asm.org/.

▽ Published ahead of print on 19 June 2009.

sumption of late differentiation to EBs, the stress response of the chlamydiae is thought to represent a suitable in vitro model for persistent infection (1, 2, 4, 25).

We have previously proposed a model for chlamydial development that reconciles many of the observations outlined above (26, 35). Two essential features of the model are the replication of RBs in type III secretion (T3S)-mediated contact with the CIM and the disruption of T3S activity through physical detachment from the CIM, which is associated with RB to EB differentiation. This so-called "contact-dependent" model has several important theoretical implications. First, an RB that actively translocates T3S effector proteins through the CIM (i.e., an RB tethered to the CIM) should not differentiate into an EB. Second and correlated to the first, an RB whose T3S system remains active for extended periods of time, by definition, should represent a persisting chlamydial cell. Biomathematical simulations predict two situations under which detachment of RBs from the CIM is physically restricted: the case of normal size RBs in a small, tight inclusion and that of abnormally large RB(s) in normal size inclusions (17, 35). The biological relevance of these simulations lies in the frequent occurrence of multiple small or lobar inclusions, e.g., for *Chlamydia pneumoniae* and *Chlamydia caviae*, in a single infected cell and the observation of stress-induced mRBs, respectively. In either case, because of the imposed spatial constraints, disruption of contact-induced T3S activity through physical RB detachment becomes a statistical rarity as the RB/mRB size approaches that of the inclusion that contains it. Remarkably, therefore, the observed in vitro persistence is not only a prediction of the biomathematical model but an implication of it as well.

We now present experimental evidence using innovative real-time light microscopy that provides some support to the contact-dependent hypothesis in its most fundamental aspects. We captured images of *C. trachomatis*-infected McCoy cells at key times during development using a Richardson RTM3 microscope optimized for live-cell imaging in extreme dark field (28). Live images were obtained with a high-resolution color analogue output video camera and recorded with Volocity software (Improvision, Coventry, United Kingdom). Taped imaging sequences were captured in Final Cut Pro and converted to Quicktime movies. We then analyzed these movies to obtain the spatial time-dependent trajectories of the movement of individual chlamydial particles in each infected cell, allowing kinematic calculations of the displacement and speed of individual particles.

MATERIALS AND METHODS

Live microscopy in the RTM3. We used the Richardson RTM3 microscope that allows capture of very-high-resolution (>50 nm) images under real-time conditions, facilitated by design improvements including an extremely light-tight and ultraclean design, removal of stray wavelengths (UV and near-infrared), reduced vibration, and capture of images via an electronic detector rather than the human eye (29). An extreme-dark condenser, infinity-corrected 100× oil objective (1.4 numerical aperture), and images captured to tape through a three-chip charge-coupled-device camera gave a resolution of 640 by 480 pixels (National Television System Committee standard). Live imaging was simultaneously viewed on a high-resolution broadcast monitor (tape capture) and on a MacIntosh G4 (still images or time-lapse capture with Volocity software; Improvision, Coventry, United Kingdom).

Living infected and mock-infected McCoy cells were imaged at various times postinfection. Semiconfluent McCoy monolayers seeded in two-chambered slides (one chamber uninfected) were infected with *C. trachomatis* serovar K/UW-31 at a multiplicity of infection of ~1. Alternatively, cells in one chamber were exposed to penicillin G at 24 hpi. Times were selected to distinguish early through mature inclusions. Imaging of one representative inclusion at each developmental time was captured on DVCPro tape (30 frames/s and 30 mB/frame), and individual images were captured using Volocity software (Improvision, Inc.). Tape segments were converted to Quick Time movies with Final Cut Pro. Duplicate slides were prepared at specific developmental times and fixed for immunofluorescence assay or immunoperoxidase staining for direct comparison with images of unfixed cells.

TABLE 1. Summary of particle speed statistics based on observations at various times during development

Expt type and time course (hpi)	No. of particles tracked	Mean avg particle speed (SE [μm/s])	Min avg particle speed (μm/s)[a]	Max avg particle speed (μm/s)[b]
Control				
0	15	0.62 (0.03)	0.42	0.97
8	11	0.93 (0.11)	0.42	1.60
14	67	1.10 (0.07)	0.31	3.28
16	17	2.74 (0.37)	0.15	5.08
18	16	2.68 (0.35)	0.31	5.30
20	23	2.26 (0.33)	0.49	5.94
24	49	9.02 (0.89)	1.15	28.83
31	30	8.02 (1.03)	0.99	22.45
40	53	4.43 (0.27)	0.29	10.27
42	27	7.94 (0.83)	1.88	18.78
44	37	6.75 (0.38)	2.10	10.71
49	29	4.49 (0.45)	0.61	8.85
Penicillin treatment				
48[c]	160	3.68 (0.11)	0.50	6.27

[a] Min, minimum.
[b] Max, maximum.
[c] At 24h after penicillin treatment.

Tracking of chlamydiae. We chose a section of each movie of 10- to 100-s duration in which focus was optimal (inspection by eye). One movie was recorded for each time point, and tracked particles were confined to a single inclusion in the recorded movie. Each frame was extracted to a separate tagged-image file format (using Blaze Media Pro, version 7.0). A computer-coded loop in Matlab, version 7.3.0 (R2007b), with the Image Processing Toolbox imported each frame in succession, and the frames were converted from RBG color format to inverted grayscale images. Particles in each frame were identified according to the level of white intensity relative to the background intensity of color in neighboring pixels after calibration of the algorithm's color intensity threshold level for particle detection. Each particle location, in Cartesian pixel coordinates, was determined based on the color intensity in all neighboring pixels. Visual inspection of the algorithm output of particle locations on the images of each frame confirmed the accurate identification of particles. Once the particles were located for each frame, a list of scrambled particle locations at consecutive frames was sorted, and particles were matched between frames (this computationally intensive procedure was based on the maximum plausible displacement in any time interval a particle could move, taken to be 15 pixels per 1/30-s time interval between frames, and accounted for the possible appearance and disappearance of particles, in and out of focus, between frames). This provided a complete description of each particle's two-dimensional time-dependent trajectory. Not all particles in each inclusion could be analyzed because it was not possible to identify unique particles that were highly clustered near others, particularly in regions in which cell debris and other material obscured the view. All particles that could be clearly identified within the optimal resolution attainable and could be tracked over at least five frames (0.17 s) were included in the analysis; particles that were identified as moving in and out of the plane of focus were excluded. Particles were tracked for as long as possible, up to the duration of the movie section analyzed (10 to 100 s). The numbers of particles included at each time point are indicated in Table 1. Elementary kinematic properties (displacement and speed) were then calculated.

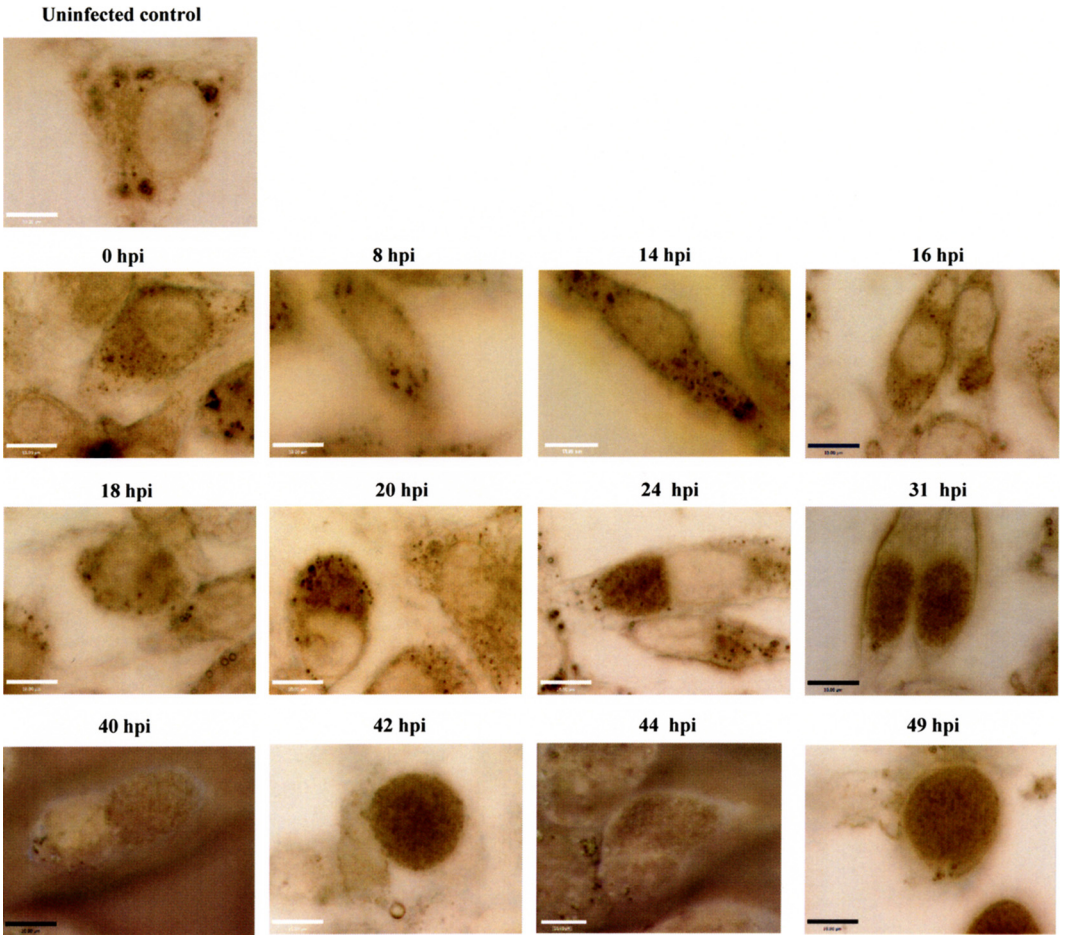

FIG. 1. Representative still image frame from each time point recorded by our RTM live imaging during normal development. Cells are unstained and viewed under RTM image contrast. Times 40 and 44 hpi are shown in differential interference contrast mode. Bar, 10 μm.

RESULTS

Movement of chlamydial particles is related to development. In Fig. 1, we display still images of *C. trachomatis*-infected McCoy cells at times representative of stages of chlamydial development (for corresponding video recordings, see Videos S1 to S12 in the supplemental material). Although visualization of nascent inclusions is not possible using this methodology, newly internalized (or surface-attached) EBs were clearly identified by comparison with uninfected cells (Fig. 1, compare uninfected cells and cells at 0 hpi). At later developmental stages, the inclusion became increasingly distinguishable owing to the higher light refraction of densely packed inclusions and to the differential velocity of chlamydiae within the inclusion compared to cytosolic contents. EBs/IBs and RBs were recognizably distinct, respectively, as densely centered particles of diameter ranging from 0.2 to 0.3 μm and as hollow-centered particles ranging from 0.6 to 1.0 μm. The slight difference between these measurements and accepted sizes (0.25 μm and 0.8 to 1.0 μm, respectively) most likely results from the diffuse boundaries between EBs/IBs and IBs/RBs and/or from the dark-field illumination method used for observation. In some instances, single particles were highly mobile in the plane of observation, but in other cases, movement was unobservable. The degree of particle movement differed widely: at one extreme, RBs were primarily immobile with only occasional episodes of wobbling movement; at the other extreme, most EBs were rapidly mobile. In between these two extremes were intermediate-size particles assumed to be in the process of differentiation to EBs. We quantified these observations through analysis of the recorded real-time video of *C. trachomatis*-infected McCoy cells. For each movie, we tracked the trajectory of individual chlamydial particles over time (Fig. 2). The average speed of each particle over the time of tracking was determined. We found that the average particle speed changed over the time course of the developmental cycle (Fig. 3A and Table 1), consistent with the observations of high EB mobility and in-place RB wobbling.

Wobbling of RBs in place increases during exponential growth. During the early to middle stages of development, there are only RBs (8 to 16 hpi) or a mixture of RBs and IBs (16 to 20 hpi). We calculated that the average speed of RBs was 0.93 μm/s (mean over all particles; standard error [SE], 0.11 μm/s) at 8 hpi, 1.10 μm/s (0.07 μm/s ± SE) at 14 hpi, and 2.74 μm/s (0.37 μm/s ± SE) at 16 hpi (Fig. 3A and Table 1). The maximum speed of the fastest particle observed at these times was 8.69 μm/s at 16 hpi. The magnitudes of these speeds

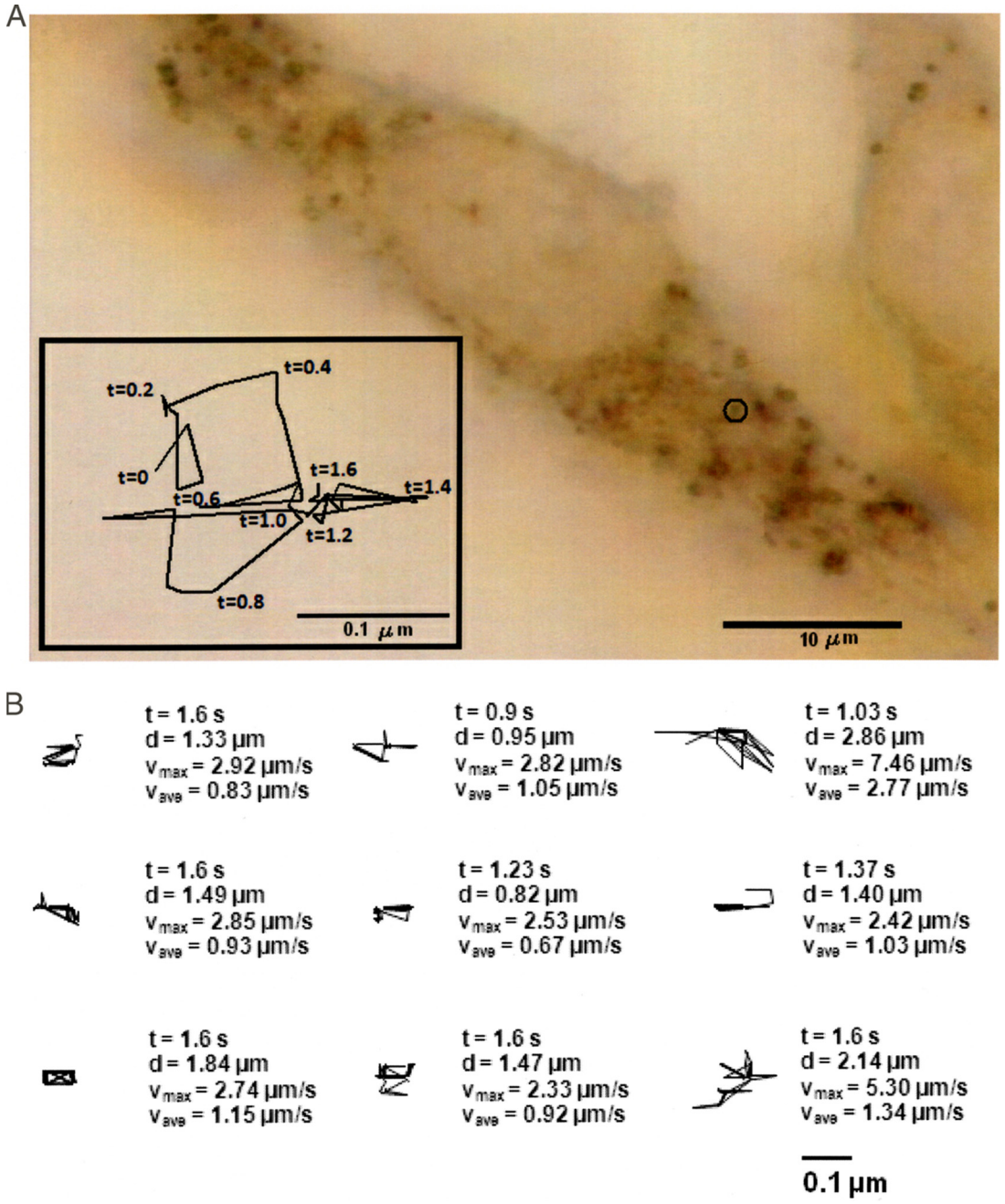

FIG. 2. (A) The trajectory over 1.6 s of the movement of the center of one representative chlamydial particle at 14 hpi in an unstained infected McCoy cell (at 100 times the original magnification). The center of this particle moved a distance of 1.28 μm in 1.6 s (i.e., with an average speed of 0.8 μm/s). (B)Tracking of nine individual particles indicating elapsed time, distance traveled, maximum velocity, and average velocity for the case of normal development (without the addition of penicillin) at 14 hpi. *t*, time; *d*, distance.

are very small relative to the size of the RB particles and in comparison with the speed of the small EBs (Table 1). Moreover, the maximum displacement (maximum distance between two points of a particle's trajectory) traveled by RBs up to 20 hpi was below the distance corresponding to the RB radius (average displacement of RBs was 0.18 μm, and the maximum measured displacement over all particles before 20 hpi was 0.59 μm), reflecting the in-place wobbling of RBs. Interestingly, the (average and maximum) speed of RB particles increased with time (although the size of particles did not change).

The average speed of RB movement increases sharply at mid-cycle and then decreases. The average speed of particles increased with time until approximately 24 hpi, with a sharp upward trend between 20 and 24 hpi for approximately half of the particles analyzed (Fig. 3A). Accrued velocity did not correlate with a significant change in particle size as size was

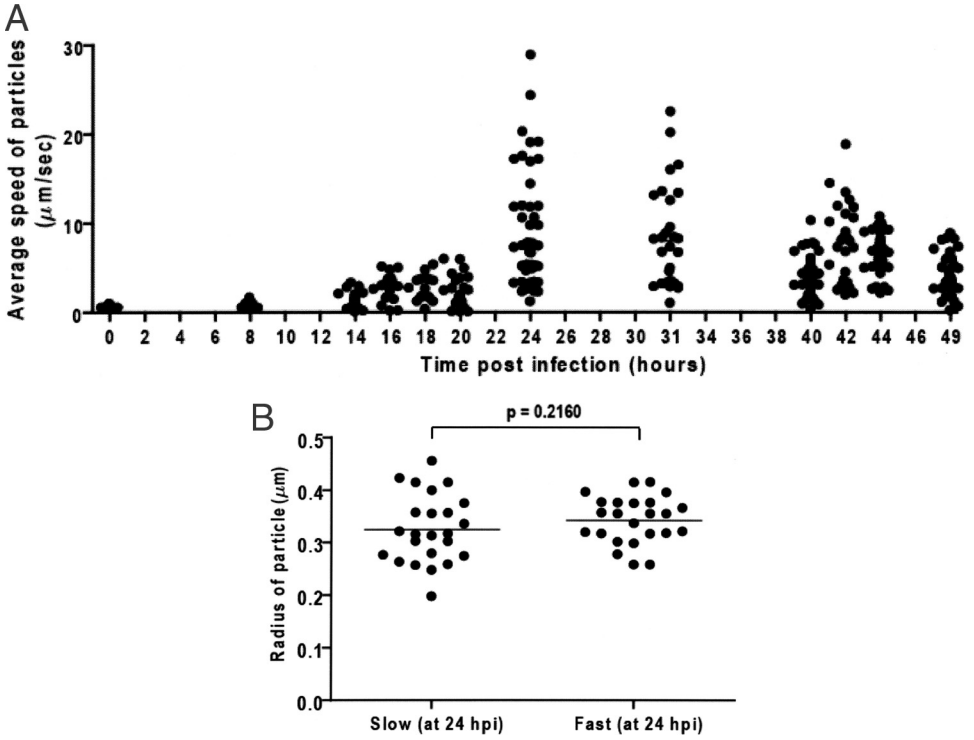

FIG. 3. (A) Average speed of chlamydial particles at each time point in the developmental cycle. (B) Univariate scatter plot. Particles tracked at 24 hpi were separated into two groups based on whether the average particle speed was greater or less than the median average speed, and the radii of chlamydial particles in the fast versus slow groups are compared. The *P* value refers to a Mann-Whitney statistical test.

randomly distributed across all particles tested at 24 hpi (Fig. 3B) ($P = 0.2160$; Mann-Whitney test based on categorizing all particles tracked at 24 hpi according to whether their average speed was greater than or less than the median particle's speed of 7.23 μm/s). At 24 hpi the mean average speed of particles was 9.02 μm/s, and the maximum average speed observed was 28.83 μm/s. Moreover, chlamydial particles at 24 hpi not only displayed accrued average speed but also traveled distances within the inclusion several times greater than the RB radius, consistent with the presumed untethering of these particles from the CIM between 20 and 24 hpi. The 24 hpi time point coincides with the time at which a substantial proportion of RBs are undergoing differentiation, and there is still sufficient physical space within the inclusion to allow maximal movement. After this point in the developmental cycle, the average speed per particle decreases (Fig. 3A and Table 1). The number of chlamydial particles and proportion that have become IBs or EBs increase with time; consequently, the space available for their movement decreases (Fig. 1).

Penicillin-induced persistent forms are static. To further explore the influence of particle size on particle motion, we investigated the movement properties of stress-induced mRBs that are known to persist under in vitro culture conditions. In this experiment, *C. trachomatis*-infected McCoy cells were exposed to 100 U/ml penicillin G at 24 hpi, and the real-time movement was recorded a further 24 h later (see the supplemental material for video recording). Under these conditions, inclusions contained a mixture of particles of sizes consistent with EBs, RBs, large penicillin-induced mRBs, and a variety of intermediate-size forms (Fig. 4A). We quantified the size and average speed of chlamydial particles of each type (Fig. 4B; see also Fig. S5 and S6 and Video S13 in the supplemental material). Particles of the size of mRBs had slower speeds (median, 0.81 μm/s; interquartile range [IQR], 0.75 to 0.88 μm/s) than RBs/I Bs (median, 1.44 μm/s; IQR, 1.15 to 2.05 μm/s), which were slower than EBs (median, 4.12 μm/s; IQR, 3.48 to 4.72 μm/s) (Fig. 4B). While there was clearly a significantly negative, nonlinear association between speed and particle size, we observed a rise in the average speed of RB particles (or IBs in the process of differentiation) relative to mRBs and an even more substantial rise for EBs. The association between speed and particle size was apparent and was statistically significant; however, it should be noted that the sample size around the cutoff between EBs and RBs was relatively small (Fig. 4B). The near immobility of mRBs is consistent with the possibility that they remain tethered to the inclusion membrane. We also compared the speeds of particles consistent with the size of EBs (Fig. 4B) with the speeds of particles in the normal development experiments at 49 hpi so that, for the comparisons, it is at a similar time postinfection that the majority of particles in the normal development experiment were EBs. We found that speeds of EBs in the penicillin-treated culture were not statistically different from those in the untreated culture ($P = 0.4624$, Mann-Whitney test); however, the treated culture had slightly lower average speeds (median of 4.1 μm/s compared with 4.4 μm/s).

DISCUSSION

We have previously proposed a hypothesis for the development of intracellular chlamydiae based on a combination of

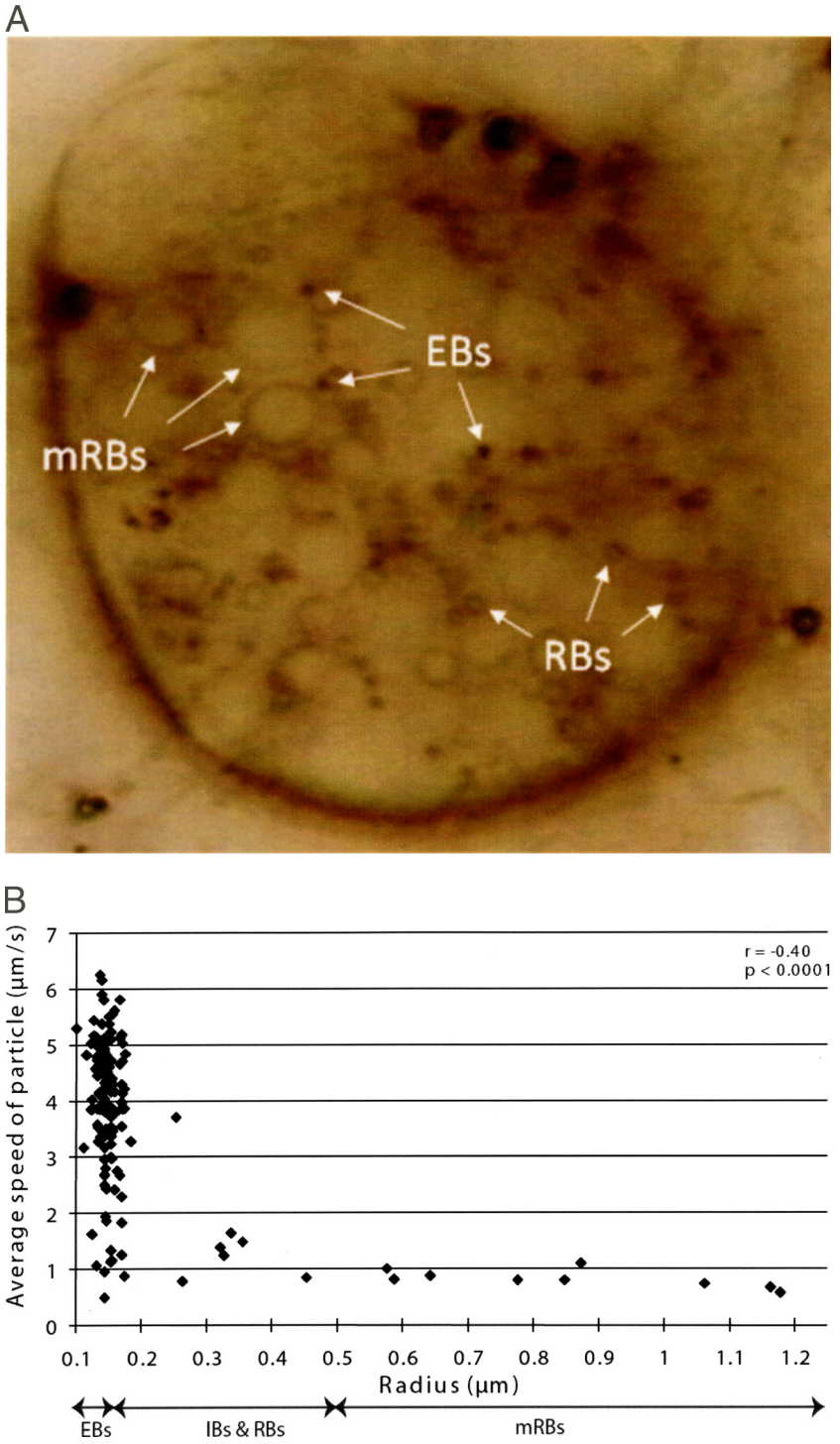

FIG. 4. (A) Still image from live video imaging of a *C. trachomatis*-infected McCoy cell (48 hpi) exposed to penicillin (100 U/ml added at 24 hpi). Cells are unstained and viewed under RTM image contrast (100 times the original magnification). Sample EBs, RBs, and mRBs are indicated. Bar, 10 μm. (B) Average velocity of chlamydial particles versus particle radius in an inclusion of a *C. trachomatis*-infected McCoy cell (48 hpi) exposed to penicillin (24 hpi). The Spearman correlation coefficient between velocity and particle size was determined (*r*; with *P* value).

electron microscopic and other observations (26) and further developed the hypothesis using biomathematical modeling (35). Tenets of the so-called contact-dependent hypothesis of chlamydial development are the following: (i) as RBs, chlamydiae grow strictly in contact with the plasma membrane-derived CIM, (ii) contact with the CIM is mediated by surface projections hypothesized to correspond to T3S injectisomes, and (iii) disruption of T3S activity through physical detach-

ment from the CIM is associated with the onset of late differentiation. The implied biological significance of the hypothesis is that maintaining contact with the CIM permits continued delivery of chlamydial T3S effectors into the host cell cytosol and subsequent subversion of cellular processes to benefit chlamydial growth; moreover, disruption of contact through physical detachment interrupts T3S effector translocation, thus rendering the host cell less hospitable for chlamydial growth. Because contact of chlamydial particles with the CIM, or loss thereof, has direct implications on the ability of chlamydiae to move inside the inclusion, we sought to quantify the movement (distance traveled and velocity) of individual chlamydial particles at different times along development. For this analysis, we used a Richardson RTM3 light microscope (28, 29) that is optimized for high-resolution white-light microscopy and live recording (30 frames per s) of *Chlamydia*-infected cells in real time. There are some limitations to the quantification of movement. (i) The movies are a cross-sectional, two-dimensional slice of the infected cells, and so particles that move in and out of focus are difficult to track. We have made allowances for this in our image-processing computer algorithms, but if fast-moving particles move far when out of focus, then identification and matching of particles are prevented. (ii) During late stages of development, the inclusion lumen is densely packed with EBs, and spatial constraints are likely to prevent unhindered movement. The high density at late stages also makes it difficult to distinguish some particles between frames. To alleviate this problem we included only particles for which we could clearly identify and match particles between frames. (iii) We could not record the same cell for each stage of the developmental cycle included in our analysis. We recorded representative cells in the culture at each time point. We acknowledge that there would be some asynchrony of infection or development and that there may be some differences at times where the same phenotypes are seen.

The results of our analysis reveal a close relationship between key developmental stages and motion properties of the chlamydiae. While movement of chlamydial bodies has been noted previously (22), this is the first detailed study using advanced microscopic techniques to (i) confirm that chlamydiae definitely do undergo movement and (ii) link this movement to specific stages of development. The magnitude and speed of RB wobbling from early to middle stages of development (Fig. 3A, 8 to 20 hpi) steadily increase with time, suggesting that individual RBs gradually lose contact with the CIM, allowing for increased movement and reciprocally supporting their hypothesized tethering to the CIM via T3S injectisomes. This is consistent with the observation that the number of surface projections decreases during development, as observed by Matsumoto in *C. psittaci* (20). Between 20 and 24 hpi, a remarkable gain in movement is observed for approximately half of the particles in an inclusion such that average velocities of individual particles are approximately four times greater at 24 hpi than at 20 hpi (Table 1). Coincidentally, the distances traveled by individual particles are substantially increased. These results are consistent with the contact-dependent hypothesis whereby untethering of individual particles is predicted to be asynchronous during late differentiation.

Naturally, larger-sized particles will move at a slower rate than smaller particles when acted upon by the same force. It is, therefore, predictable that the decreasing size of the chlamydial particle (from 0.8 to 1.0 μm for the RB to 0.25 μm for the EB) will affect the degree of movement during late differentiation. However, we found that the fastest particles in the developmental cycle (at 24 hpi) were of the size of RB particles (Fig. 3B). Given the very marked change observed from essentially no movement or slight in-place wobbling of RBs to very fast motion of newly detached RBs, IBs, or EBs, we conclude that the large gain of velocity observed between 20 and 24 hpi is not accounted for significantly by the change in the size of the chlamydial particle as it undergoes late differentiation. A steady decrease in speed was also observed between 24 and 49 hpi, i.e., during late differentiation. We speculate that particles gradually lose velocity as they bounce off each other and off the CIM in the increasingly crowded inclusion lumen. Biomathematical simulations of the contact-dependent hypothesis predict that both the multiplicity of inclusions within a single infected cell and the size of the chlamydial particle relative to that of the inclusion are determining factors in the outcome of an infection (17, 35). In multiple, smaller inclusions within an infected cell, the size differential between the inclusion and that of a replicating RB it contains may become small enough such that loss of T3S-mediated contact between the RB and the CIM becomes improbable. Following the same logic, the likelihood of an extremely large RB's becoming untethered from the CIM diminishes with increasing RB size. We explored this part of the hypothesis using *C. trachomatis* grown in the presence of penicillin. Penicillin-exposed chlamydial cultures are known to produce aberrantly enlarged mRBs and provide a model for chlamydial persistence, a hallmark of chlamydial chronic infection and disease in humans (1, 2, 4, 25). In our experiments, cultures were supplemented with penicillin G at 24 hpi and observed at 48 hpi, allowing for inclusions to contain a mixture of persistent mRBs as well as normal RBs, IBs, and EBs. We found that EBs in inclusions exposed to penicillin moved at maximal speeds similar to those observed at 49 hpi in normal cultures (Fig. 4B and Table 1). Particles the size of RBs were observed to wobble in place, while mRBs were either completely static or wobbled slightly in place. This is consistent with the idea that these particles are more extensively tethered to the underlying CIM and suggests that mRBs may not become untethered from the CIM, with the consequence that they do not enter late differentiation and that they persist de facto. Hence, the motion properties of chlamydial particles within persistent inclusions are consistent with the results of biomathematical simulations that predict that mRBs persist in vitro owing to their continued tethering to the CIM. Although this hypothesis ultimately requires experimental verification, it is consistent with gene expression studies that have shown at both the transcriptional and protein levels that expression of the T3S injectisome genes is not significantly affected during persistent growth (5, 24).

The T3S system is thought to be central to the virulence of many bacterial pathogens including *Chlamydia* spp. (11, 19, 26). However, there is no consensus as to whether a functional T3S system exists during the intracellular growth phase of chlamydiae and, if so, whether tethering of each single RB to the inclusion membrane via T3S injectisomes is necessary for

development. A role of T3S in chlamydial pathogenesis is supported by virulence-related properties of several chlamydial T3S-translocated effectors (7, 8, 33). Other studies have coupled T3S expression or T3S activity with development (12, 32, 36). An attractive hypothesis emerging from these converging results is that T3S-mediated translocation of early mid-cycle effector(s) to the infected cell cytosol maintains the host in a state optimized for chlamydial exponential growth and that disruption of this state through interruption of T3S translocation may "alert" chlamydiae within the inclusion to initiate late differentiation and subsequent progress of the infection. Stress-induced inhibition of this process would then represent a survival mechanism of the chlamydiae whereby a sustained level of T3S translocation activity maintains viability of fewer chlamydiae but for extended periods of time. Although our study does not directly address T3S activity and its potential role in development, our findings are consistent with the contact-dependent hypothesis. Further experiments beyond the scope of this study would be required to investigate the potential role of the T3S system on chlamydial development. Our novel approach of using real-time light microscopy and kinetics analysis with *Chlamydia* has described chlamydial movement in a way that has never been done previously. It has elucidated properties in the regulation of the unique developmental cycle of this medically important pathogen.

ACKNOWLEDGMENTS

These studies were supported by NHMRC CDA568705 (D.P.W.), NHMRC project support (P.T.), and NIH grants AR48331 (J.W.-H.), AI54310, and AI51417 (P.M.B.). The National Centre in HIV Epidemiology and Clinical Research is funded by the Australian Government Department of Health and Ageing.

We thank Kelley Hovis for providing supporting confocal microscopy. We thank Shuxiang Goh for image processing support and Tim Richardson and the staff of Richardson Technologies, Inc., for the opportunity and training to investigate chlamydial biology under real-time conditions.

REFERENCES

1. **Al-Younes, H. M., T. Rudel, V. Brinkmann, A. J. Szczepek, and T. F. Meyer.** 2001. Low iron availability modulates the course of *Chlamydia pneumoniae* infection. Cell Microbiol. **3:**427–437.
2. **Beatty, W. L., T. A. Belanger, A. A. Desai, R. P. Morrison, and G. I. Byrne.** 1994. Tryptophan depletion as a mechanism of gamma interferon-mediated chlamydial persistence. Infect. Immun. **62:**3705–3711.
3. **Beatty, W. L., G. I. Byrne, and R. P. Morrison.** 1993. Morphologic and antigenic characterization of interferon gamma-mediated persistent *Chlamydia trachomatis* infection in vitro. Proc. Natl. Acad. Sci. USA **90:**3998–4002.
4. **Beatty, W. L., R. P. Morrison, and G. I. Byrne.** 1995. Reactivation of persistent *Chlamydia trachomatis* infection in cell culture. Infect. Immun. **63:**199–205.
5. **Belland, R. J., D. E. Nelson, D. Virok, D. D. Crane, D. Hogan, D. Sturdevant, W. L. Beatty, and H. D. Caldwell.** 2003. Transcriptome analysis of chlamydial growth during IFN-gamma-mediated persistence and reactivation. Proc. Natl. Acad. Sci. USA **100:**15971–15976.
6. **Cevenini, R., M. Donati, and M. La Placa.** 1988. Effects of penicillin on the synthesis of membrane proteins of *Chlamydia trachomatis* LGV2 serotype. FEMS Microbiol. Lett. **56:**41–46.
7. **Chellas-Gery, B., C. N. Linton, and K. A. Fields.** 2007. Human GCIP interacts with CT847, a novel *Chlamydia trachomatis* type III secretion substrate, and is degraded in a tissue-culture infection model. Cell Microbiol. **9:**2417–2430.
8. **Clifton, D. R., K. A. Fields, S. S. Grieshaber, C. A. Dooley, E. R. Fischer, D. J. Mead, R. A. Carabeo, and T. Hackstadt.** 2004. A chlamydial type III translocated protein is tyrosine-phosphorylated at the site of entry and associated with recruitment of actin. Proc. Natl. Acad. Sci. USA **101:**10166–10171.
9. **Coles, A. M., D. J. Reynolds, A. Harper, A. Devitt, and J. H. Pearce.** 1993. Low-nutrient induction of abnormal chlamydial development: a novel component of chlamydial pathogenesis? FEMS Microbiol. Lett. **106:**193–200.
10. **Fields, K. A., E. R. Fischer, D. J. Mead, and T. Hackstadt.** 2005. Analysis of putative *Chlamydia trachomatis* chaperones Scc2 and Scc3 and their use in the identification of type III secretion substrates. J. Bacteriol. **187:**6466–6478.
11. **Fields, K. A., and T. Hackstadt.** 2006. The *Chlamydia* type III secretion system: structure and implications for pathogenesis, p. 219–233. *In* P. M. Bavoil and P. B. Wyrick (ed.), *Chlamydia* genomics and pathogenesis. Horizon Bioscience, Norfolk, United Kingdom.
12. **Fields, K. A., D. J. Mead, C. A. Dooley, and T. Hackstadt.** 2003. *Chlamydia trachomatis* type III secretion: evidence for a functional apparatus during early-cycle development. Mol. Microbiol. **48:**671–683.
13. **Hackstadt, T., W. Baehr, and Y. Ying.** 1991. *Chlamydia trachomatis* developmentally regulated protein is homologous to eukaryotic histone H1. Proc. Natl. Acad. Sci. USA **88:**3937–3941.
14. **Hackstadt, T., E. R. Fischer, M. A. Scidmore, D. D. Rockey, and R. A. Heinzen.** 1997. Origins and functions of the chlamydial inclusion. Trends Microbiol. **5:**288–293.
15. **Hackstadt, T., D. D. Rockey, R. A. Heinzen, and M. A. Scidmore.** 1996. *Chlamydia trachomatis* interrupts an exocytic pathway to acquire endogenously synthesized sphingomyelin in transit from the Golgi to the plasma membrane. EMBO J. **15:**964–977.
16. **Hackstadt, T., M. A. Scidmore, and D. D. Rockey.** 1995. Lipid metabolism in *Chlamydia trachomatis*-infected cells: directed trafficking of Golgi-derived sphingolipids to the chlamydial inclusion. Proc. Natl. Acad. Sci. USA **92:**4877–4881.
17. **Hoare, A., P. Timms, P. M. Bavoil, and D. P. Wilson.** 2008. Spatial constraints within the chlamydial host cell inclusion predict interrupted development and persistence. BMC Microbiol. **8:**5.
18. **Hsia, R.-C., H. Ohayon, P. Gounon, A. Dautry-Varsat, and P. M. Bavoil.** 2000. Phage infection of the obligate intracellular bacterium *Chlamydia psittaci* strain GPIC. Microbes Infect. **2:**761–772.
19. **Hsia, R.-C., Y. Pannekoek, E. Ingerowski, and P. M. Bavoil.** 1997. Type III secretion genes identify a putative virulence locus of *Chlamydia*. Molecular Microbiology **25:**351–359.
20. **Matsumoto, A.** 1982. Electron microscopic observations of surface projections on *Chlamydia psittaci* elementary bodies. J. Bacteriol. **150:**358–364.
21. **Matsumoto, A.** 1981. Isolation and electron microscopic observations of intracytoplasmic inclusions containing *Chlamydia psittaci*. J. Bacteriol. **145:**605–612.
22. **Matsumoto, A.** 1988. Structural characteristics of chlamydial bodies, p. 21–45. *In* A. L. Barron (ed.), Microbiology of *Chlamydia*. CRC Press, Inc., Boca Raton, FL.
23. **Matsumoto, A., and G. P. Manire.** 1970. Electron microscopic observations on the effects of penicillin on the morphology of *Chlamydia psittaci*. J. Bacteriol. **101:**278–285.
24. **Molestina, R. E., J. B. Klein, R. D. Miller, W. H. Pierce, J. A. Ramirez, and J. T. Summersgill.** 2002. Proteomic analysis of differentially expressed *Chlamydia pneumoniae* genes during persistent infection of HEp-2 cells. Infect. Immun. **70:**2976–2981.
25. **Peters, J., S. Hess, K. Endlich, J. Thalmann, D. Holzberg, M. Kracht, M. Schaefer, G. Bartling, and A. Klos.** 2005. Silencing or permanent activation: host-cell responses in models of persistent *Chlamydia pneumoniae* infection. Cell Microbiol. **7:**1099–1108.
26. **Peters, J., D. P. Wilson, G. Myers, P. Timms, and P. M. Bavoil.** 2007. Type III secretion á la *Chlamydia*. Trends Microbiol. **15:**241–251.
27. **Peterson, E. M., and L. M. de la Maza.** 1988. *Chlamydia* parasitism: ultrastructural characterization of the interaction between the chlamydial cell envelope and the host cell. J. Bacteriol. **170:**1389–1392.
28. **Pham, N. A., M. R. Gal, R. D. Bagshaw, A. J. Mohr, B. Chue, T. Richardson, and J. W. Callahan.** 2005. A comparative study of cytoplasmic granules imaged by the real-time microscope, Nile Red and Filipin in fibroblasts from patients with lipid storage diseases. J. Inherit. Metab. Dis. **28:**991–1004.
29. **Pham, N. A., T. Richardson, J. Cameron, B. Chue, and B. H. Robinson.** 2004. Altered mitochondrial structure and motion dynamics in living cells with energy metabolism defects revealed by real time microscope imaging. Microsc. Microanal. **10:**247–260.
30. **Raulston, J. E.** 1997. Response of *Chlamydia trachomatis* serovar E to iron restriction in vitro and evidence for iron-regulated chlamydial proteins. Infect. Immun. **65:**4539–4547.
31. **Scidmore-Carlson, M. A., E. I. Shaw, C. A. Dooley, E. R. Fischer, and T. Hackstadt.** 1999. Identification and characterization of a *Chlamydia trachomatis* early operon encoding four novel inclusion membrane proteins. Mol. Microbiol. **33:**753–765.
32. **Slepenkin, A., V. Motin, L. M. de la Maza, and E. M. Peterson.** 2003. Temporal expression of type III secretion genes of *Chlamydia pneumoniae*. Infect. Immun. **71:**2555–2562.
33. **Stenner-Liewen, F., H. Liewen, J. M. Zapata, K. Pawlowski, A. Godzik, and J. C. Reed.** 2002. CADD, a *Chlamydia* protein that interacts with death receptors. J. Biol. Chem. **277:**9633–9636.

34. **Tamura, A., and G. P. Manire.** 1968. Effect of penicillin on the multiplication of meningopneumonitis organisms (*Chlamydia psittaci*). J. Bacteriol. **96:**875–880.
35. **Wilson, D. P., P. Timms, D. L. McElwain, and P. M. Bavoil.** 2006. Type III secretion, contact-dependent model for the intracellular development of *Chlamydia*. Bull. Math. Biol. **68:**161–178.
36. **Wolf, K., H. J. Betts, B. Chellas-Gery, S. Hower, C. N. Linton, and K. A. Fields.** 2006. Treatment of *Chlamydia trachomatis* with a small molecule inhibitor of the *Yersinia* type III secretion system disrupts progression of the chlamydial developmental cycle. Mol. Microbiol. **61:**1543–1555.
37. **Wolf, K., E. Fischer, and T. Hackstadt.** 2000. Ultrastructural analysis of developmental events in *Chlamydia pneumoniae*-infected cells. Infect. Immun. **68:**2379–2385.